

Geology of the crystalline basement of the Hadbin area (Salalah area, Dhofar, Sultanate of Oman)

Autor(en): **Hauser, André / Zurbriggen, Roger**

Objektyp: **Article**

Zeitschrift: **Schweizerische mineralogische und petrographische Mitteilungen
= Bulletin suisse de minéralogie et pétrographie**

Band (Jahr): **74 (1994)**

Heft 2

PDF erstellt am: **25.04.2024**

Persistenter Link: <https://doi.org/10.5169/seals-56343>

Nutzungsbedingungen

Die ETH-Bibliothek ist Anbieterin der digitalisierten Zeitschriften. Sie besitzt keine Urheberrechte an den Inhalten der Zeitschriften. Die Rechte liegen in der Regel bei den Herausgebern.

Die auf der Plattform e-periodica veröffentlichten Dokumente stehen für nicht-kommerzielle Zwecke in Lehre und Forschung sowie für die private Nutzung frei zur Verfügung. Einzelne Dateien oder Ausdrucke aus diesem Angebot können zusammen mit diesen Nutzungsbedingungen und den korrekten Herkunftsbezeichnungen weitergegeben werden.

Das Veröffentlichen von Bildern in Print- und Online-Publikationen ist nur mit vorheriger Genehmigung der Rechteinhaber erlaubt. Die systematische Speicherung von Teilen des elektronischen Angebots auf anderen Servern bedarf ebenfalls des schriftlichen Einverständnisses der Rechteinhaber.

Haftungsausschluss

Alle Angaben erfolgen ohne Gewähr für Vollständigkeit oder Richtigkeit. Es wird keine Haftung übernommen für Schäden durch die Verwendung von Informationen aus diesem Online-Angebot oder durch das Fehlen von Informationen. Dies gilt auch für Inhalte Dritter, die über dieses Angebot zugänglich sind.

Geology of the crystalline basement of the Hadbin area (Salalah area, Dhofar, Sultanate of Oman)

by André Hauser and Roger Zurbriegen¹

Abstract

The Salalah area is an erosional window in the sedimentary cover of the crystalline basement of the Arabian shield. The Hadbin area is situated in the eastern part of the Salalah area. The Proterozoic crystalline basement of the Hadbin area can be divided into three complexes.

The *Sadh complex* consists of highly deformed and migmatitic rocks with a polymagmatic and polymetamorphic history. Field relations, macroscopic and microscopic observations and geochemistry point to plutonic protoliths of this complex which forms the country rock of the plutons: Fusht and Hadbin complexes.

The *Fusht complex* consists of a suite of dioritic to tonalitic rocks which suffered syn- to post-magmatic deformation. The mantle-derived magma ascended during extensional tectonics and was not contaminated by crustal rocks.

The younger *Hadbin complex*, ranging from quartz diorite to granodiorite in composition, emplaced after deformation. The more acid magmas of the Hadbin complex, compared with those of the Fusht complex, are explained by crustal contamination of mantle-derived calc-alkaline magmas. Geochemical calculations show that leucogranitic material generated in deeper levels of the migmatitic Sadh complex is a possible source of these crustal melts.

Keywords: Proterozoic, calc-alkaline plutonism, crustal contamination, Arabian shield.

1. Introduction

This paper presents the geology and petrography of the Hadbin area, incorporating results from microscopy, ore microscopy, X-ray diffraction and X-ray fluorescence. In addition we propose a magmatic model for the development of the Hadbin area.

Most of the crystalline basement of the Arabian shield is exposed in the west of Saudi Arabia and Yemen. In the eastern part of the Arabian Peninsula it is entirely covered with sediments, except for some smaller erosional windows located in Oman. The largest of the windows is located in the Salalah area (Fig. 1). Hitherto, the Salalah area has been only superficially investigated, even though it presents a well exposed region to examine the Proterozoic and early Phanerozoic crustal evolution of the eastern Arabian shield. Absolute age determinations in the crystalline basement of the Salalah area by GASS et al. (1990)

and FREI et al. (in prep.) show late Proterozoic ages. Paleozoic clastic sediments (BEYDUN, 1966) discordantly overlie the crystalline basement and are covered discordantly by horizontally-bedded Cretaceous and Tertiary calcareous sediments of the Umm Er Rhadhuma formation (ROGER and PLATEL, 1987).

Previous workers (MMAJ, JICA and GJ, 1981) carried out a geologic and radiometric survey as part of their ore exploration. Their map (scale 1 : 100'000) distinguishes a plutonic "granodioritic Hadbin body" and the "Sadh gneiss" representing the country rock of the former. Based on detailed mapping at 1 : 23'000 scale (HAUSER and ZURBRIGGEN, 1992) we have subdivided their "granodioritic Hadbin body" into the Fusht and the Hadbin complexes. Another part of the former "Hadbin body" we have mapped as leucocratic gneisses of the Sadh complex.

In particular, the excellent outcrops and the lack of any post-magmatic, penetrative deforma-

¹ Mineralogisch-Petrographisches Institut der Universität Bern, Baltzerstrasse 1, CH-3012 Bern, Switzerland.

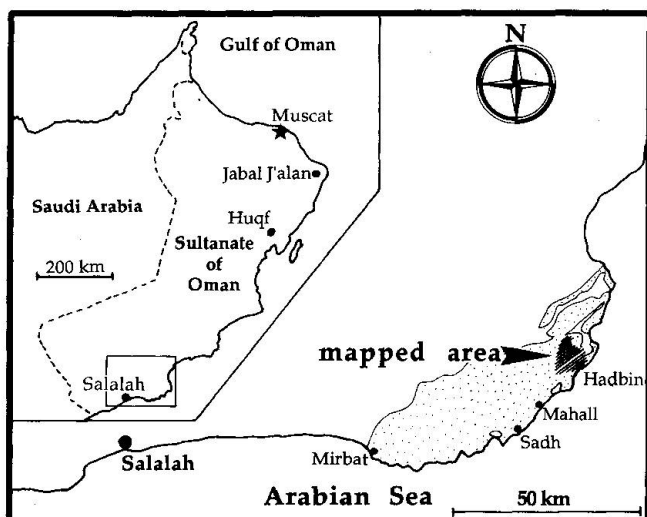


Fig. 1 Map of the Sultanate of Oman. The spotted area represents the outcropping crystalline basement. The hatched part is the investigated Hadbin area.

tion allows original magmatic features to be studied well. As a result we have been able to develop a model for the magmatic evolution of the Hadbin area. This study is restricted to the Hadbin area, the most eastern part of the Salalah area. The crystalline basement of the Salalah area as a whole was investigated by WÜRSTEN (1994).

2. The country rock: Sadh complex

2.1. LITHOLOGIES AND AGE RELATIONS

The Sadh complex is characterized by a strong lithological banding on all scales. The bands are oriented parallel to the penetrative foliation and strike generally E–W in the southern area, whereas in the northern area the structures are aligned parallel to the contacts with the Fusht complex and the Hadbin complex (Fig. 2). Upper amphibolite facies metamorphism is indicated by the abundance of migmatites. Based on structural relationships the Sadh complex can be divided into three units consisting of similar lithologies (Tab. 1) which have been intruded into each other.

(i) The *most deformed* rocks in the Sadh complex are composed of banded gneiss (alternating bands of leucocratic gneiss, biotite-hornblende gneiss and amphibolite thinner than 20 m) and biotite-hornblende gneiss grading continuously into each other. Concordant bands of leucocratic gneiss and amphibolite are interlayered in the previous series (Figs 2 and 3). (ii) The second *less deformed* unit is composed of large, homogeneous rock bodies of metadiorite and leucocratic

gneiss. They are oriented mainly parallel, but also discordant, to the gneiss structures (Figs 2 and 3). Both contain enclaves of the first group. Metadioritic enclaves within the leucocratic gneiss and original plutonic contacts are interpreted as the intrusion of a leucocratic magma into a metadiorite. The deformation is most intense at the rim of the bodies whereas in the center the plutonic fabric have often remained unaffected. This is illustrated by metadiorite grading into amphibolite at the rims. (iii) The third group of *undeformed* leucogranitic apophyses, dykes and agmatites (Fig. 3) cross-cut all other rocks of the Sadh complex. They are interpreted to be a product of the last migmatization of the Sadh complex.

2.2. PROTOLITHS

In the field, no metasediments (metacarbonates or metapelites) were found, and likewise, the geochemistry shows no clear evidence for metasediments (HAUSER and ZURBRIGGEN, 1992). Therefore it seems likely that the protoliths are of magmatic origin.

The isotropic fabric and the intrusive contacts of metadiorite and leucocratic gneiss are strong indications of a plutonic origin of these rock types. For the most deformed rock types (banded gneiss and biotite-hornblende gneiss with interlayered bands of leucocratic gneiss and amphibolite) the question regarding the protolith is more difficult to answer. The plutonic microfabric, and the absence of metasediments indicating deep crustal levels, point to a plutonic origin. The strong banding is formed by the intense shearing of magmatic structures. In places the banding can be explained by partial anatexis or metamorphic segregation.

Because all lithologies of the Sadh complex show the same chemical and mineralogical trends but variable textures, they can be interpreted as repeated series of calc-alkaline plutonic rocks which reflect a common origin but different relative ages, and therefore different deformation histories.

3. The plutons: Fusht and Hadbin complexes

3.1. FUSHT COMPLEX

Earlier works in this area (Report of MMAJ, JICA and GJ, 1981) did not interpret the Fusht rocks as a distinct complex, but they mapped them as Hadbin intrusives. In map view the Fusht complex is an elliptic, north-south oriented plutonic body. It

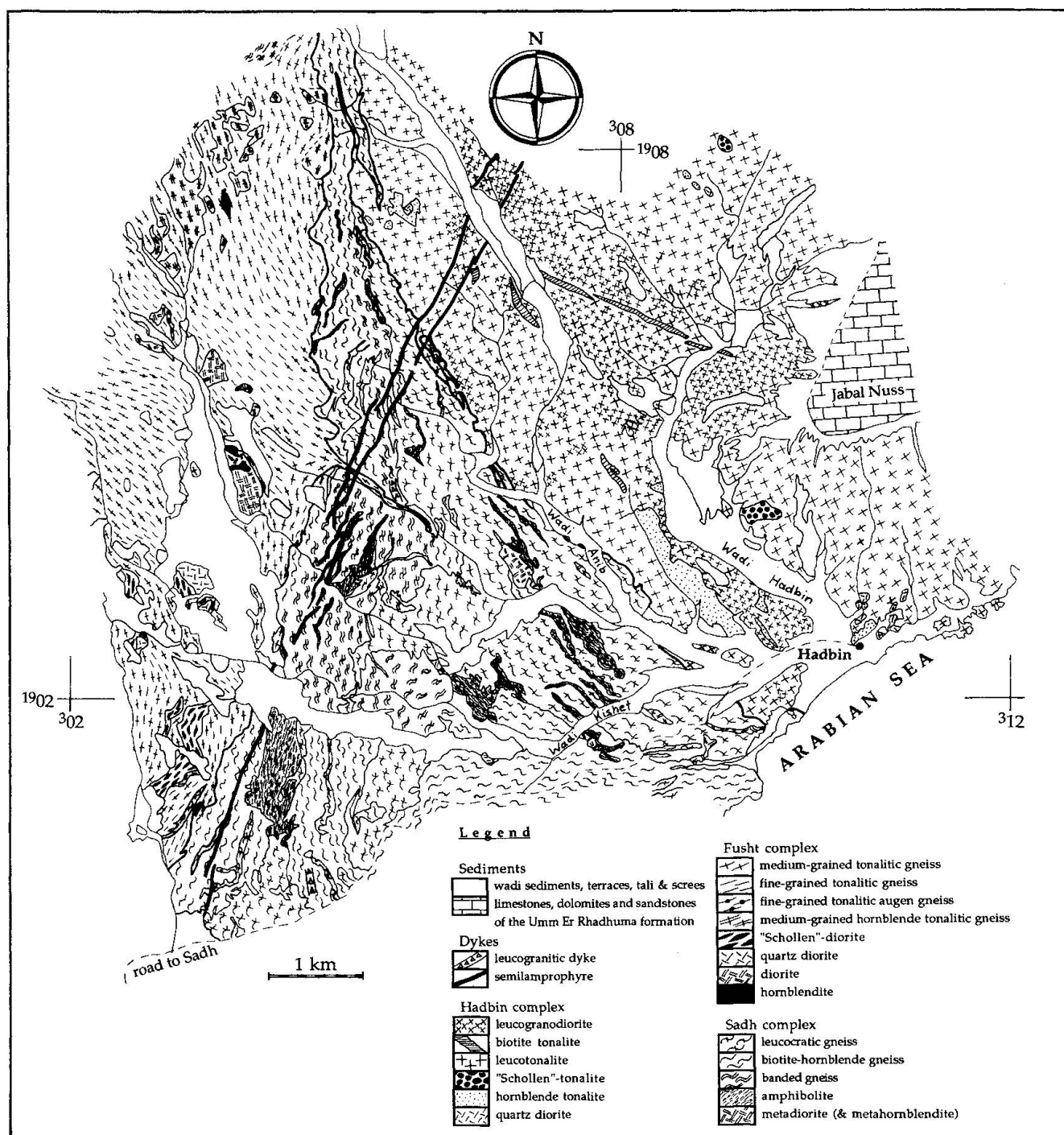


Fig. 2 Geologic map of the Hadbin area.

consists mainly of tonalitic (trondhjemitic) gneisses (90%) and minor dioritic rocks. Where schistosity is lacking the Fusht tonalites look very similar to the younger undeformed Hadbin rocks. The general orientation of the schistosity in the mapped part of the Fusht complex is 250/30 (dip azimuth / dip angle), which is concordant to the magmatic contact and the internal structures of the host rocks (the Sadh complex). The observations that this concordance occurs all along the

contact of the Fusht complex, and the schistosity is best developed in the margin of the pluton (WURSTEN, 1994) could be explained by emplacement tectonics in the lower crust (ballooning). The schistosity is deformed by open folds with interlimb distances of 1–10 m. The fold axes are subhorizontal and strike NW–SE $\pm 45^\circ$.

The Fusht complex is composed of the eight following rock types. Their compositions are given in table 1. The main lithology is a *medium-*

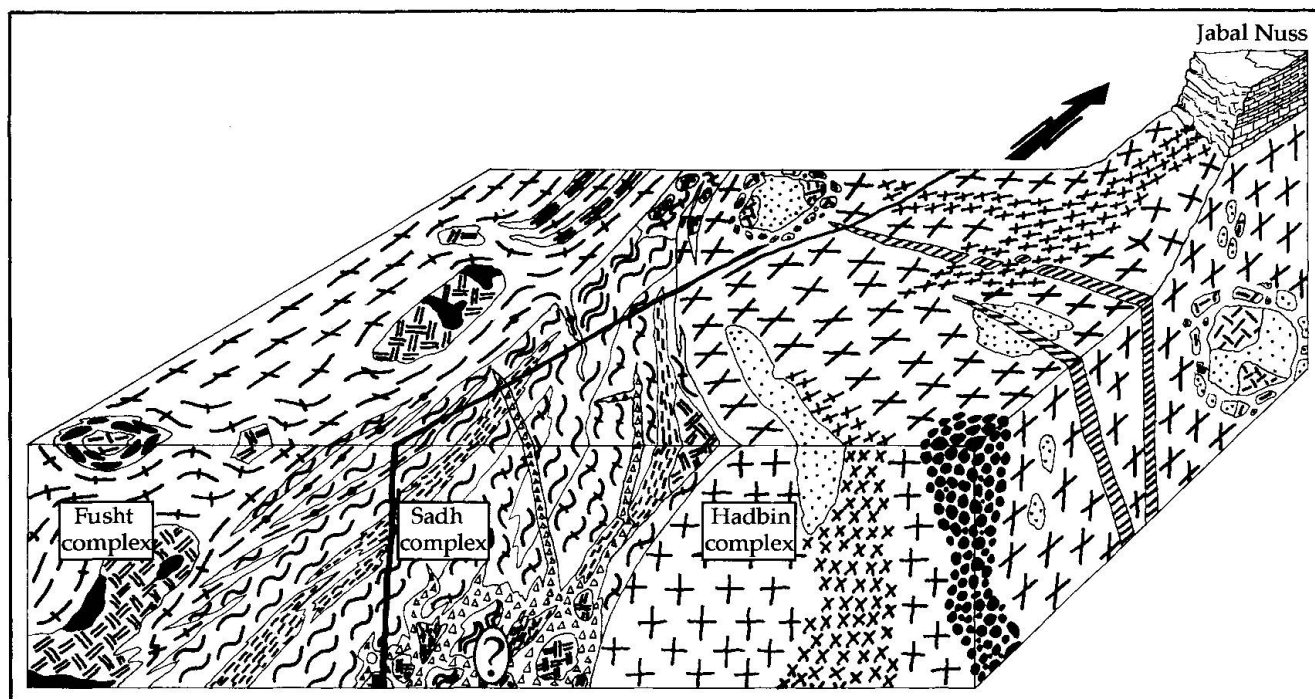


Fig. 3 Schematic block diagram of the Hadbin area. The lithologies and their relationships are described in the text. (For legend see figure 2.)

grained tonalitic gneiss (i) with a granular texture. Biotite, hornblende, plagioclase phenocrysts and elongated quartz grains are subparallel and define the schistosity. The *fine-grained tonalitic gneiss (ii)* and the *fine-grained tonalitic augen gneiss (iii)* are textural varieties of the main lithology. The augen type contains biotite free patches (~ 1 cm in diameter) in the center of which euhedral titanite (partly resorbed) is situated. This unusual texture is of magmatic origin but not yet understood in detail. The *medium-grained hornblende tonalitic gneiss (iv)* is a hornblende-richer variety of the main lithology. It forms huge concordant slabs within the main rock (Fig. 3). The "Schollen"-diorite (v) consists of about two thirds of cm-m sized fine-grained (quartz-) dioritic enclaves (so-called "Schollen") which are imbedded in a medium-grained quartz dioritic to hornblende tonalitic matrix. This rock is generated by the intermingling of dioritic and tonalitic magmas. The elongated dark "Schollen" in the light matrix produce a strong gneissic character. The *quartz diorite (vi)* is always associated with the "Schollen"-diorite (Figs 2 and 3). Medium-grained *diorite (vii)* occurs as up to 800 m long bodies. A similar diorite occurs as angular enclaves in the tonalitic gneisses. We do not know if these enclaves are endogenous or exogenous. In the latter case they might be xenoliths of the Sadh-metadiorites. Smaller bodies of *hornblendite (viii)* occur within the diorites.

The lack of cross-cutting relationships lead us to the interpretation that the various rock types crystallized contemporaneously. In this view, the generation of the tonalitic and dioritic magmas can be explained by fractional crystallization of the same parental magma (Fig. 5). The dioritic magmas accumulated in the lower part of the Fusht-magma chamber. Convection induced mixing and mingling of dioritic with "stratigraphically higher" tonalitic magmas (yielding "Schollen"-diorite) within the zone of hybridization where the present erosional surface lies.

Dioritic and tonalitic dykes intruded the Fusht complex and the neighboring Sadh complex prior to emplacement of the Hadbin complex. These dykes belong to the magmatism of the Fusht complex. They cross-cut already foliated tonalites of the Fusht complex and are thus further evidence for syn-magmatic tectonics.

Xenoliths of the Sadh complex are very rare in the Fusht complex. This indicates that the present erosional surface intersects the Fusht pluton at an intermediate to lower level, otherwise roof pendant of the Sadh complex would be more common.

3.2. HADBIN COMPLEX

In contrast to the Fusht complex, the Hadbin complex is undeformed, and it is possible to determine an internal sequence of intrusion (Fig. 3).

Tab. 1 Modal composition of the rock types of the Sadh, Fusht, and Hadbin complexes. General accessory minerals are: apatite, zircon, allanite, epidote, titanite, rutile, magnetite, ilmenite, and hematite. (Numbers in brackets refer to the amount of specimens. Abbreviations: Qtz, quartz; Pl, plagioclase; Kfs, K-feldspar; Bt, biotite; Hbl, hornblende.)

complex			modal composition (vol.%)				
rock type			Qtz	Pl	Kfs	Bt	Hbl
H A D B I N	leucogranodiorite (3)		32–46	36–47	14–18	2–5	–
	biotite tonalite (2)		22–27	58–60	0–1	12–19	–
	"Schollen"- tonalite	matrix (1)	~ 18	~ 75	–	~ 7	–
		"Schollen" (2)	3–17	53–61	–	18–30	5–10
	leucotonalite (10)		15–38	53–66	< 8	4–9	–
	hornblende tonalite (5)		17–21	54–63	–	9–20	< 8
	quartz diorite (4)		5–14	41–49	–	4–19	23–44
F U S H T	medium-grained tonalitic gneiss (7)		13–31	51–68	0–2	10–18	0–2
	fine-grained tonalitic gneiss (3)		16–21	64–71	–	9–12	0–1
	fine-grained tonalitic augen gneiss (4)		~ 16	~ 67	< 2	~ 12	–
	medium-grained Hbl-tonalitic gneiss (2)		13–17	~ 57	0–1	11–18	8–13
	"Schollen"- diorite	matrix (1)	~ 6	~ 70	–	~ 6	~ 17
		"Schollen" (1)	–	~ 52	–	~ 7	~ 38
	quartz diorite (4)		3–12	52–69	–	0–24	0–42
	diorite (2)		–	34–39	–	–	59–65
S A D H	hornblendite (1)		–	12	–	–	85
	undef.	leucogranitic dyke (2)	33–35	31–34	30–34	< 1	–
	less deformed	leucocratic gneiss (4)	15–35	53–75	1–15	< 6	–
		metadiorite (3)	0–2	34–62	–	< 1	19–51
	most deformed	amphibolite (7)	0–18	33–58	–	0–21	13–41
		biotite-hornblende gneiss (10)	14–35	48–67	0–16	3–17	0–24
		leucocratic gneiss (5)	20–36	42–72	4–26	< 3	–
		banded gneiss		bands of leucocratic gneiss, Bt-Hbl gneiss and amphibolite			

The Hadbin complex consists of six, fine- to medium-grained rock types ranging in composition from quartz diorite to granodiorite (for modal data see table 1). The main lithology (80%) is a *leucotonalite* (i). The *quartz diorite* (ii) is the basic end-member of the magmatic suite and is often associated with the *hornblende tonalite* (iii), whereas the former occurs as enclaves in the latter. Both lithologies form swarms of enclaves within the leucotonalite. The "Schollen"-tonalite (iv) can be considered as analogous to the "Schollen"-diorite of the Fusht complex (section 3.1), whereas the compositions of the "Schollen" range from dioritic to tonalitic. The formation of this rock type is attributed to intrusion of mafic magma into leucotonalitic magma. The *biotite tonalite* (v) cross-cuts the leucotonalite as dykes, whereas in some places contact relationships point to a syn-magmatic intrusion relative to the leucotonalite. Finally, the *leucogranodiorite* (vi) forms irregularly shaped bodies within the leucotonalite and cross-cuts the biotite tonalite.

The Hadbin complex is strongly interfingering with the Sadh complex, which is interpreted as an

intrusive contact. Mapping this contact was quite difficult because of similarities between the leucotonalite of the Hadbin complex and the leucocratic gneisses of the Sadh complex. All structures within the Hadbin complex (e.g., schlieren, aligned biotite, elongated and oriented rock bodies and enclaves) occur mainly along the contact with the Sadh complex and can be explained by magmatic flow processes.

The Hadbin complex is a calc-alkaline differentiation suite, whereas a part of the evolution can be explained by fractional crystallization processes. Abundant mafic and felsic schlieren within the leucotonalite and the presence of the "Schollen"-tonalite indicate that mixing and mingling of different magmas might have played an important role during the magmatic evolution of the Hadbin complex.

The order of emplacement is not identical with the QAPM*-evolutionary trend from more mafic to leucocratic lithologies (Fig. 4). This might indicate that the relative significance of various magmatic differentiation processes such as replenishing, fractionation, crustal contamination, and mix-

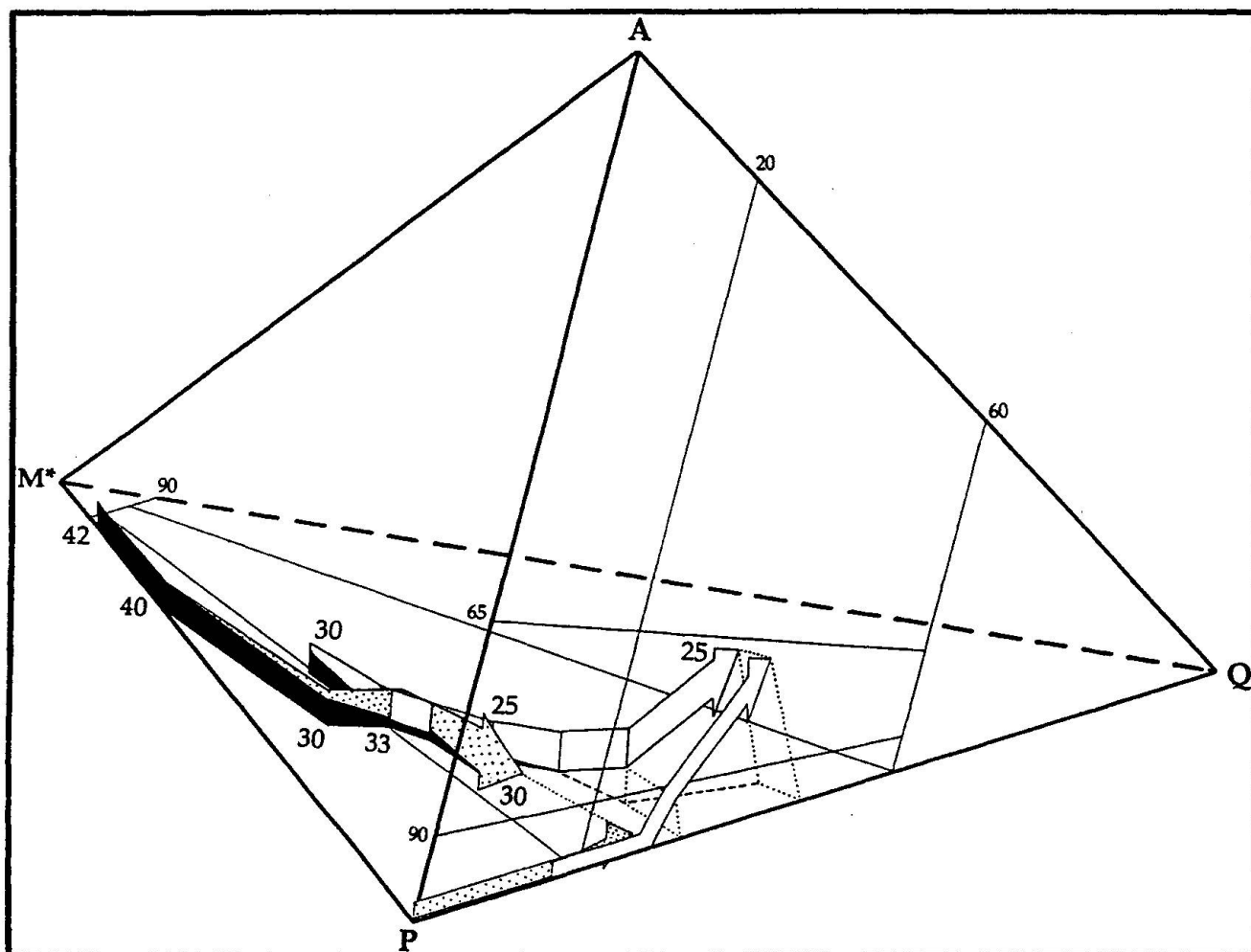


Fig. 4 QAPM*-diagram. This tetrahedron is an extended version of the QAP-modal diagram after STRECKEISEN (1975). M*: hornblende + biotite. Small numbers refer to the grid lines. Large numbers indicate the anorthite component of the plagioclase. The 42-40-30-33-30 suite belongs to the Fusht complex (large dotted arrow) and the other ones to the Hadbin complex (large white arrow). The small arrows on the Q-A-P-plane are projections (from the M*-edge) of the large arrows in the Q-A-P-M*-tetrahedron. The dashed line on the Q-P-M*-plane (not the Q-M*-line) is a projection (from the A-edge) of the large white arrow. The black component of the large arrows represents the hornblende : biotite ratio (e.g.: all black denotes no biotite, only hornblende; half black and half white/dotted denotes hornblende : biotite ratio ≈ 1 . For explanations see chapter 3.3 and table 2.)

ing were not continuous in time and space (chapter 4). All three complexes are cross-cut by granitoid dykes which are interpreted as belonging to the late magmatic episodes of the Hadbin complex.

3.3. COMPARISON AND CLASSIFICATIONS OF THE FUSHT AND HADBIN COMPLEXES

The rocks of the Hadbin and Fusht complexes are composed almost entirely of plagioclase (P), K-feldspar (A), quartz (Q), biotite and hornblende (M*). Therefore, the QAPM*-diagram (Fig. 4) demonstrates both the whole-rock miner-

alogy of the rocks and the differentiation trends of both plutonic complexes very well. In table 2 the most important mineralogical differences of both plutons are listed. Generally, the rocks of the Hadbin complex contain more quartz and much more K-feldspar (up to 15 vol.%) than those of the Fusht complex.

Geochemical data of some representative rocks are given in table 3. Figure 5 shows an Al_2O_3 - SiO_2 Harker variation diagram, which demonstrates the most important geochemical characteristics.

Generally, rocks of the Hadbin complex are the richest in SiO_2 . The diorite of the Fusht complex is the basic end-member of the main differ-

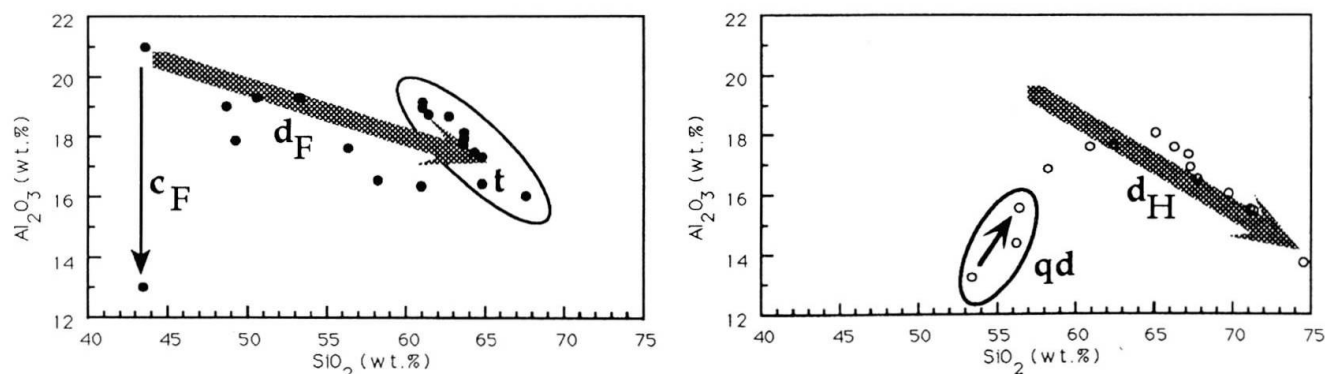


Fig. 5 Al_2O_3 - SiO_2 variation diagrams for the Fusht complex (left) and for the Hadbin complex (right). c_F : cumulate building process in the Fusht complex; d_F : main differentiation trend of the Fusht complex; t : group of tonalitic gneisses of the Fusht complex; qd : quartz diorites of the Hadbin complex; d_H : main differentiation trend of the Hadbin complex. (For explanations see chapter 3.3.)

entiation trend d_F ; The hornblendite is interpreted as the cumulate c_F , the diorite as the residual of the same parental magma. This separation into a hornblende-rich cumulate and a plagioclase-rich residual is reflected in the Al_2O_3 contents. The linear relationship of SiO_2 and Al_2O_3 in the tonalitic gneisses (t in Fig. 5) of the Fusht complex is caused by variable plagioclase modal content. The main differentiation trend (d_F) cannot solely be explained by plagioclase-amphibole fractionation, since the K_2O contents are nearly constant indicating additional biotite fractionation.

The quartz diorites (qd) of the Hadbin complex can be regarded as cumulates in analogy to the hornblendite in the Fusht complex, or as basic end-members of the main trend, which show passive enrichment in Al due to the fractionation of hornblende. This hornblende-dominated fractionation is reflected by an increase of quartz, plagioclase, and biotite from quartz diorite to biotite tonalite (Tab. 1). The main trend in the Hadbin complex (d_H) from biotite tonalite to leucogranodiorite is characterized by the absence of amphibole, decrease of biotite, and increase of quartz and K-feldspar (Tab. 1). The resulting decrease in Al_2O_3 can be explained by fractionation of biotite and plagioclase. The general early precipitation of amphibole in both plutons indicates high $p\text{H}_2\text{O}$, and, therefore, great depth of emplacement (lower to middle crust) which is in agreement with the migmatitic state of the country rocks.

Both, the Fusht and the Hadbin complexes can be classified according to LAMEYRE and BOWDEN (1982) as calc-alkaline trondhjemitic (low-K) series. In the Hadbin complex however, biotite fractionation was less important allowing precipitation of K-feldspar and the evolution towards leucogranodiorites (Fig. 4).



As we have seen, it is possible to explain the magmatic evolution of the Hadbin complex fully by fractional crystallization. On the other hand, field observations, petrographical features, and chemical whole rock analyses show that processes such as crustal contamination and hybridization must be considered as well (chapter 4).

According to the nomenclatures of ISHIHARA (1981) and PEARCE et al. (1984), the Fusht and Hadbin complexes are both calc-alkaline, magnetite series and of the volcanic-arc type and are therefore interpreted as subduction-related.

The classification scheme of CASTRO et al. (1991) is very suitable for the plutons of the Hadbin area. The Fusht complex consists mainly of mantle-derived tonalites and is therefore classified as an M-type, whereas the Hadbin complex represents a crustal contaminated H_m -type (hybrid with dominant mantle character). The $\text{K}_2\text{O}/\text{Na}_2\text{O}$ -ratio is a chemical criterion to distinguish M- and H_m -types from H_{ss} -types (hybrid granitoid sensu stricto). M- and H_m -types contain more Na_2O than K_2O , whereas H_{ss} -types have about equal amounts of Na_2O and K_2O . Note that the Hadbin-rocks plot closer to the " $\text{K}_2\text{O}=\text{Na}_2\text{O}$ -line" which reflects their hybrid character (Fig. 6). This contamination is also expressed in a relative enrichment of the rocks of the Hadbin complex in lithophile elements (e.g., Si, Na, K, Rb, Ba) compared to similar lithologies in the Fusht complex.

The alignment of the structures of the Sadh complex parallel to the contacts of the plutons points to ductile behaviour of the Sadh complex during emplacement of the intrusives. The ductility might be explained by amphibolite facies conditions and the presence of partial melts. These partial melts possibly correspond to the crustal component contaminating the ascending mantle-

Tab. 2 Differences between lithologies of the Fusht and the Hadbin complexes (cf. figure 4).

complex topics	Fusht 	Hadbin 
rock suite	hornblende-diorite-quartz diorite-tonalite	quartz diorite-tonalite-leucogranodiorite
basic endmember	hornblende and quartz- and biotite-free diorite	diorite with quartz and biotite
acid endmember	tonalite (with accessory K-feldspar)	leucogranodiorite (~15vol.% K-feldspar)
main rock	medium-grained tonalitic gneiss	leucotonalite
K-feldspar	All Fusht rocks contain only accessory or no K-feldspar. =>The large spotted arrow remains on the Q-P-M*-plane (-->fig. 4).	The leucotonalite (~5vol.%) and the leucogranodiorite (~15vol.%) contain K-feldspar. =>The large white arrow bends up towards the A-edge (-->fig. 4).
range of anorthite component of plagioclases	42 - 30 (hornblende) (tonalite)	30 - 25 (quartz diorite) (leucogranodiorite)
hornblende	Even in the most acid rocks hornblende is present.	Leucotonalite, leucogranodiorite and biotite tonalite contain no hornblende.
biotite	Hornblende and diorite contain no biotite.	All rocks contain biotite.
white mica	only secondary as sericite	primary muscovite and secondary sericite
allanite and magmatic titanite	Found in almost every thin section.	very rare
ore minerals	Fusht rocks contain more opaque phases than equivalent Hadbin rocks.	

derived magmas of the Hadbin complex. Note that, in this case, these crustal melts (the felsic S-type end-member of CASTRO et al., 1991) are generated by the partial melting of meta-igneous rocks of the Sadh complex, and not by the anatexis of metapelites such as in the Hercynian basement of Spain (CASTRO et al., 1991).

The present juxtaposition of the Fusht and Hadbin complexes and the lack of any evidence for relative tectonic movements between them indicates that both plutons ascended the same distance through the crust. The question arises why only one of the plutons is contaminated, whereas the other is not. Different regional tectonics are a possible explanation why the mantle-derived

magmas remained pure in the case of the Fusht complex, but were contaminated by crustal material in the case of the younger Hadbin complex. One can imagine that the Fusht complex ascended in an extensive tectonical regime within a relatively short time span. Later the Hadbin pluton intruded during a compressive phase, which transformed the tonalites of the Fusht complex into tonalitic gneisses and impaired the ascent of the Hadbin complex, but favoured its interaction with felsic crustal material. Such changes from extensional to compressional tectonics and resulting deformations within subduction-related arcs are also reported by MOORE and AGAR (1985) in the Peruvian Andes.

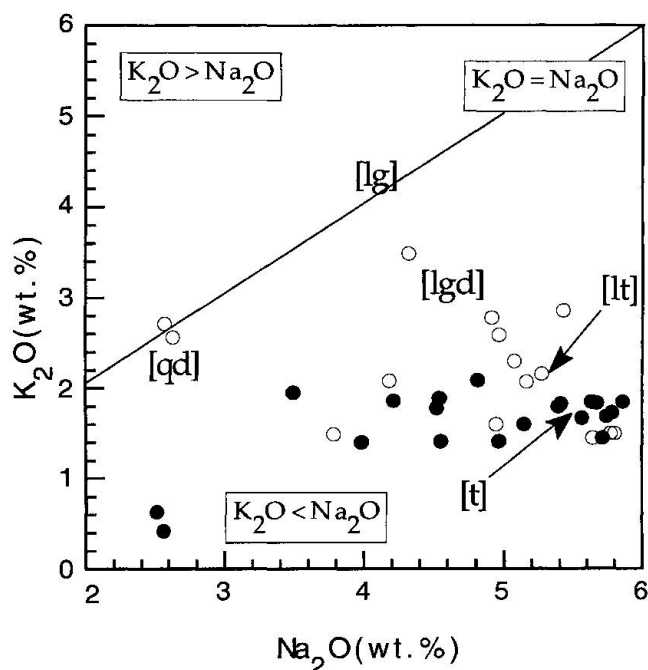


Fig. 6 K_2O - Na_2O variation diagram of the Fusht (filled circles) and Hadbin (empty circles) complexes. ([lg]: leucogranitic dyke of the Sadh complex; [lt]: leucotonalites of the Hadbin complex; [lgd]: leucogranodiorites of the Hadbin complex; [qd]: quartz diorites of the Hadbin complex; [t]: tonalitic gneisses of the Fusht complex. (For explanations see chapters 3.3. and 4.)

Another reason why only the Hadbin complex is contaminated is that it intruded a more highly migmatized Sadh complex due to the crystallization heat input of the earlier emplaced Fusht complex. This corresponds with studies by PITCHER et al. (1985) in the Coastal Batholith of Peru where highest evolved magmas are found in areas with most fully developed crust and high heat flows.

4. "Magma mixing"?

According to the classification scheme of CASTRO et al. (1991) the Hadbin complex might represent a hybride of mantle-derived magmas and crustal melts. A two-component mixing model allows the proportions of end-members to be calculated. The leucogranitic dykes [lg] which are interpreted to be a product of the last migmatization of the Sadh complex possibly represent the crustal component of a near-eutectic composition. Because the rocks of the Fusht complex are considered to be mantle derivatives they can be used in this model to represent the mantle component. The tonalitic gneisses [t] are the most acid rocks of the studied part of the Fusht complex and their vis-

cosity is the most similar to the viscosity of the leucogranitic melts, which would allow the hybridization.

The authors suppose a simple mechanical liquid-liquid mixing since all major and most of the minor elements of the mixing-participants show the same linear relationship (Tab. 4).

The mixing process can be described mathematically by a linear equation:

$$x[t] + y[lg] = [lt]$$

$$(x + y = 1 \text{ and } 0 \leq x \leq 1)$$

(1)

It follows that:

$$x = ([lt] - [lg]) / ([t] - [lg])$$

(2)

For each major-element oxide and trace element the corresponding x-value (factor of the mantle component [t]) can thus be calculated. All data and results of the calculations are listed in table 4. The mean x-value of the major element oxides is 0.69 and the median is 0.66. The low standard deviation (0.13) in the x-values means that the major elements behave in correspondence to the mixing model. A median x-value of 0.66 indicates that the leucotonalite of the Hadbin complex [lt] is theoretically a product of mixing two thirds of mantle-derived tonalitic magma [t], as found in the Fusht complex, with one third of crustal melts [lg] represented by the undeformed migmatites of the Sadh complex.

The same procedure was followed for the trace elements. The standard deviation (0.29) in the x-values is quite high, however, due to their higher analytical errors. The leucogranodiorite of the Hadbin complex can be explained by the same mixing model, but with a higher fraction of the crustal component [lg]. This is shown in figure 6 where the leucogranodiorite [lgd] lies on the [lg]-[t]-line, but closer to [lg] than [lt] does. More mafic lithologies of the Hadbin complex cannot be explained by the mixing model. This is illustrated by the quartz diorites [qd], lying onto the " $K_2O=Na_2O$ -line" in figure 6, and which are not colinear with the mixing educts [lg] and [t]. Probably too big differences in viscosity of these quartz diorites and the leucogranitic crustal melts did not allow their homogeneous mixing (hybridization). This is directly supported by the field observations that (quartz-) dioritic and (leuco-) tonalitic melts did not mix homogeneously, but intermingled to form the "Schollen"-dioritic/tonalitic rocks. This indicates that the quartz dioritic lithologies of the Hadbin complex originated mainly by fractionation processes and not by crustal contamination of even more basic diorites, as found in the Fusht complex. Thus, this mixing process was active in a very restricted range of time, during the formation of the leu-

Tab. 3 Geochemical data of representative rocks of the studied part of the crystalline basement of the Hadbin area.

Sadh complex: OS592: concordant band of most deformed leucocratic gneiss, OS593: leucocratic dyke, OS595: biotite-hornblende gneiss, OS617: amphibolite, OS628: metadiorite, OS629: metahornblende, OS921: less deformed leucocratic gneiss.

Fusht complex: OS597: "Schollen"-diorite, OS598: diorite, OS621: fine-grained tonalitic gneiss, OS650: quartz diorite, OS659: hornblende, OS860: medium-grained tonalitic gneiss, OS869: fine-grained tonalitic augen gneiss, OS967: medium-grained hornblende tonalitic gneiss.

Hadbin complex: OS564: hornblende tonalite, OS624: leucotonalite, OS776: "Schollen"-tonalite, OS877: biotite tonalite, OS914: quartz diorite. (B.d.l.: below detection limit. X-ray fluorescence analyses were done at the University of Fribourg/CH by G. Galetti.)

sample number	Sadh complex					Fusht complex					Hadbin complex				
	OS592	OS593	OS595	OS617	OS628	OS629	OS921	OS597	OS598	OS621	OS650	OS659	OS860	OS869	OS967
SiO ₂	71.94	75.52	62.93	53.53	52.19	51.38	62.00	50.57	48.68	63.63	56.34	43.47	64.33	63.66	60.96
TiO ₂	0.12	0.03	0.84	1.06	1.40	0.90	0.84	1.32	1.02	0.54	1.11	2.44	0.55	0.60	0.82
Al ₂ O ₃	16.30	14.22	16.84	14.36	16.31	10.89	19.56	19.30	19.03	17.75	17.63	13.01	17.51	18.15	16.36
Fe ₂ O ₃ total	0.96	0.24	5.37	7.94	8.02	8.68	3.99	8.83	10.14	3.70	7.21	13.13	3.77	4.03	5.98
MnO	0.02	0.01	0.08	0.12	0.11	0.15	0.17	0.16	0.15	0.08	0.11	0.14	0.08	0.08	0.09
MgO	0.28	0.10	2.43	5.64	6.82	11.64	0.94	4.16	5.77	1.70	3.62	13.73	1.33	1.47	2.94
CaO	2.67	1.53	4.23	6.03	7.95	11.61	3.01	6.90	8.05	3.99	5.73	8.54	3.78	4.00	5.02
Na ₂ O	5.79	4.07	4.71	2.71	3.49	2.13	6.42	4.52	3.49	5.39	4.55	2.56	5.63	5.67	4.54
K ₂ O	1.64	4.32	1.84	2.40	1.33	0.70	3.04	1.78	1.95	1.80	1.41	0.42	1.85	1.84	1.89
P ₂ O ₅	0.04	0.03	0.26	0.22	0.15	0.13	0.24	0.37	0.12	0.23	0.24	0.15	0.23	0.28	0.26
loss on ignition	0.33	0.17	0.48	5.55	1.88	1.35	0.23	2.00	1.87	1.11	2.02	2.42	0.53	0.52	0.70
total (wt %)	100.09	100.24	100.01	99.56	99.65	99.56	100.44	99.91	100.27	99.92	99.97	100.01	99.59	100.30	99.56
Nb	b.d.l.	b.d.l.	b.d.l.	b.d.l.	b.d.l.	b.d.l.	b.d.l.	b.d.l.	b.d.l.	b.d.l.	b.d.l.	b.d.l.	b.d.l.	b.d.l.	b.d.l.
Zr	105	66	176	74	54	49	20	130	25	123	51	62	163	197	188
Y	b.d.l.	b.d.l.	16	10	15	13	20	19	b.d.l.	6	11	12	9	b.d.l.	10
Sr	919	635	786	412	695	404	346	962	922	810	884	322	846	893	677
U	b.d.l.	b.d.l.	b.d.l.	b.d.l.	b.d.l.	b.d.l.	b.d.l.	b.d.l.	b.d.l.	b.d.l.	b.d.l.	b.d.l.	b.d.l.	b.d.l.	b.d.l.
Rb	15	33	41	59	21	11	50	34	35	34	25	4	40	33	44
Th	b.d.l.	b.d.l.	b.d.l.	b.d.l.	b.d.l.	b.d.l.	b.d.l.	b.d.l.	b.d.l.	b.d.l.	b.d.l.	b.d.l.	b.d.l.	b.d.l.	b.d.l.
Pb	8	15	b.d.l.	b.d.l.	b.d.l.	b.d.l.	b.d.l.	b.d.l.	b.d.l.	50	b.d.l.	b.d.l.	b.d.l.	b.d.l.	b.d.l.
Ga	16	14	21	17	15	14	22	20	19	17	17	12	19	19	17
Zn	18	2	72	84	70	76	62	119	107	61	84	92	63	66	71
Cu	b.d.l.	b.d.l.	b.d.l.	66	53	200	b.d.l.	31	26	b.d.l.	31	148	b.d.l.	b.d.l.	14
Ni	b.d.l.	b.d.l.	17	84	27	133	b.d.l.	8	16	b.d.l.	10	256	b.d.l.	b.d.l.	21
Co	8	12	21	39	39	47	5	28	41	14	25	62	12	11	25
Cr	b.d.l.	b.d.l.	47	271	29	378	4	22	31	8	26	584	6	9	68
V	1	4	101	200	308	239	37	188	257	51	155	363	41	47	108
Ce	27	15	68	18	21	19	29	28	b.d.l.	26	23	18	44	39	28
Nd	7	b.d.l.	24	12	15	14	b.d.l.	32	10	13	19	17	11	8	16
Ba	874	2514	873	566	521	262	5580	772	498	664	448	126	634	551	578
La	14	b.d.l.	37	11	7	b.d.l.	6	13	b.d.l.	8	6	9	21	14	16
S	b.d.l.	60	43	100	55	96	44	207	324	96	224	350	18	21	54
Hf	3	5	6	3	b.d.l.	2	b.d.l.	b.d.l.	b.d.l.	b.d.l.	b.d.l.	b.d.l.	b.d.l.	3	3
total (ppm)	2015	3375	2349	2026	1945	1957	6225	2613	2311	1981	2039	2437	1927	1911	1938
								2340	1617	1973	2659	1930			2436

Tab. 4 Composition of the hypothetical mixing members and calculations (calculated by equation 2) of mixing proportions (x-values). (For further explanations see chapter 4.)

rock type	average of tonalitic gneisses of the Fusht complex	leucogranitic dyke (OS593) of the Sadh complex	average of leucotonalites of the Hadbin complex		
symbol	[t]	[lg]	[lt]		x
SiO ₂	63.52	75.52	68.22		0.61
TiO ₂	0.61	0.03	0.35		0.55
Al ₂ O ₃	17.90	14.22	16.65		0.66
Fe ₂ O ₃ total	4.13	0.24	2.73		0.64
MnO	0.08	0.01	0.07		0.81
MgO	1.53	0.1	0.92		0.57
CaO	4.07	1.53	2.89		0.54
Na ₂ O	5.52	4.07	5.35		0.88
K ₂ O	1.76	4.32	2.18		0.84
P ₂ O ₅	0.26	0.03	0.18		0.66
l. o. i.	0.57	0.17	0.51		0.85
total (wt %)	99.94	100.24	100.03	mean	0.69
				st. dev.	0.13
				median	0.66

cotonalitic and leucogranodioritic melts. The ⁸⁷Sr/⁸⁶Sr ratio and REE patterns of these rocks might provide further evidence for or against this mixing model.

5. Discussion: an evolutionary model for the Hadbin area

The aim of this section is to combine the geological events of the three complexes into a coherent history of the Hadbin area. There is no doubt concerning the relative ages of the three complexes: the polymagmatic and polymetamorphic Sadh complex is the oldest unit intruded by the (deformed) Fusht and the younger (undeformed) Hadbin plutons. The main question is whether the geological histories of the three complexes overlap in time or not. In other words, are there any magmatic or high-grade metamorphic events which affected two or even all three complexes?

The last migmatization of the Sadh complex (**M**) is the youngest event in the Sadh complex, and produced the undeformed leucogranitic dykes and agmatites. Thus the leucogranitic dykes cross-cut all other rocks and structures of the Sadh complex. With this in mind, the timing of the last migmatization of the Sadh complex is the most critical event. One can envisage two principally different models (Fig. 7). In the "linear model" the Fusht and Hadbin complexes were emplaced post-**M**, whereas in the "interfering

model" the Fusht complex and its deformation are pre-**M** and the Hadbin magmatism syn- to post-**M**. "Variation a" and "variation b" (Fig. 7) slightly modify the linear model allowing small overlaps of the histories of the three complexes.

At the present stage of investigation the final decision between the two models cannot be made, but we favour the interfering model for the following reasons:

- Leucogranitic dykes and agmatites generated during the last migmatization of the Sadh complex (**M**) do not show signs of deformation. Therefore they must be younger than the deformation of the Fusht complex.

- The alignment of the structures of the Sadh complex parallel to the borders of both plutons indicates that the Sadh complex was ductile during the intrusion of the undeformed Hadbin complex, probably due to the presence of partial melts.

- The coexistence of migmatites and the intruding magmas of the Hadbin complex would allow processes shown by the mixing model (chapter 4).

- The absence of leucogranitic dykes in the Fusht and the Hadbin complexes seems to contradict the interfering model, but this can be explained as follows: The leucogranitic dykes form

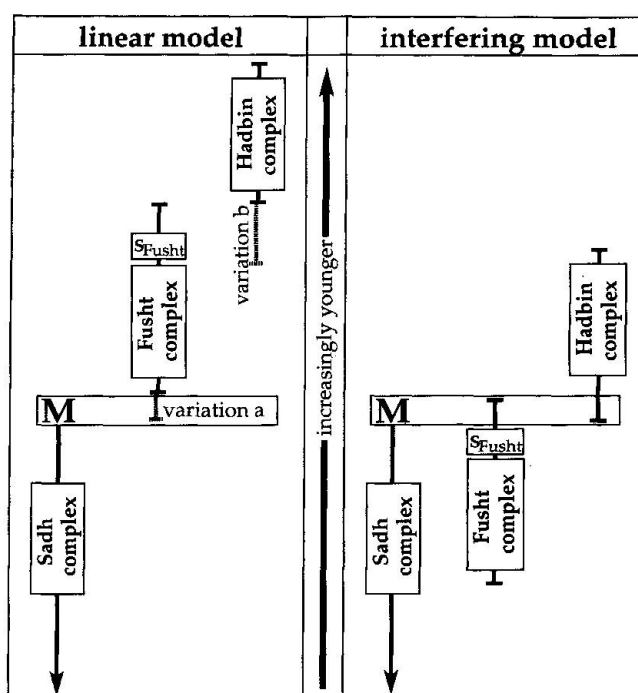


Fig. 7 Two intrusion models of the Fusht and Hadbin plutons in the Sadh complex.

(**M**: final migmatization of the Sadh complex. **S_{Fusht}**: deformation of the Fusht complex. For explanations see chapter 5.)

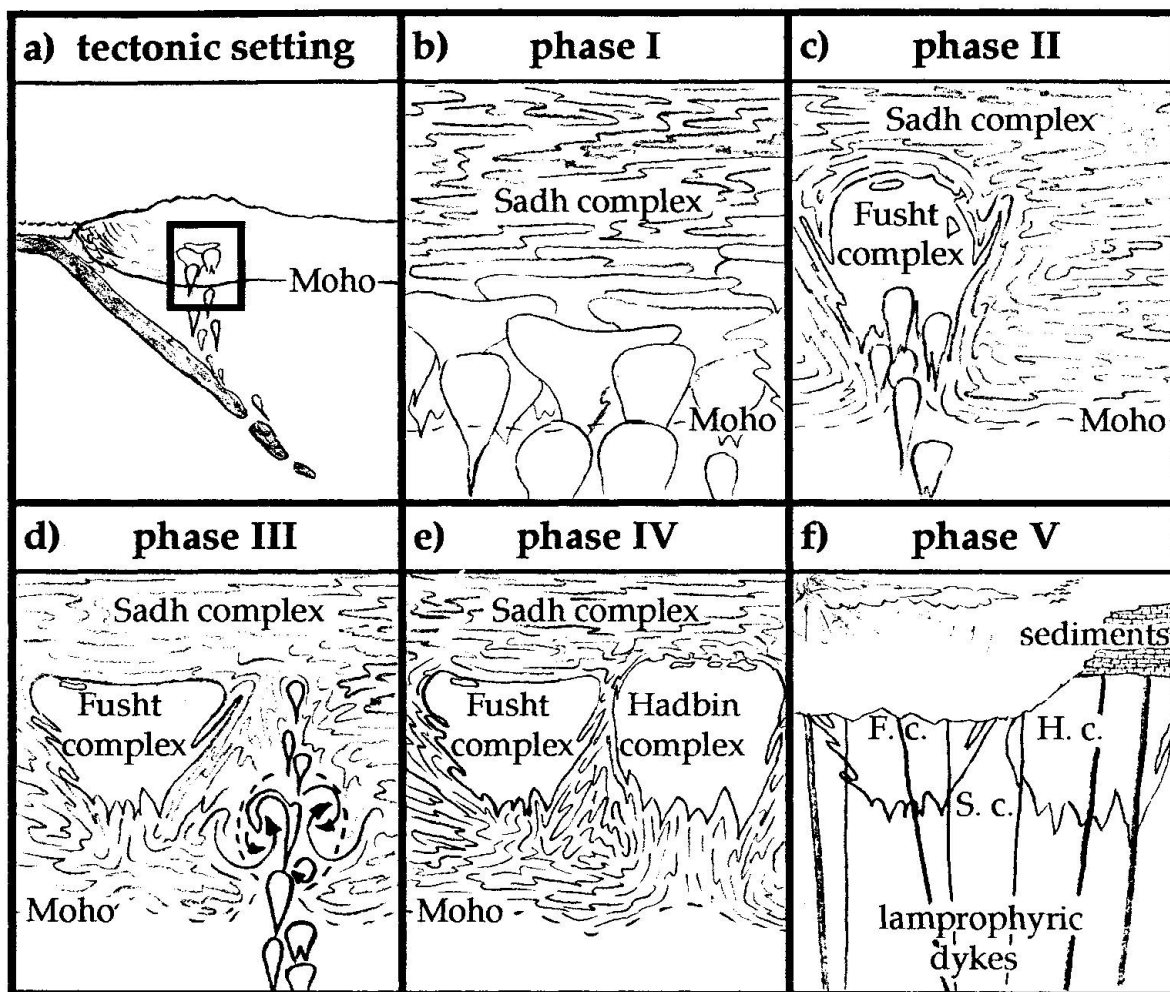


Fig. 8 a-f: Geologic history of the Hadbin area. (For explanations see chapter 5.)

discordant apophyses of larger leucosomes cross-cutting the adjacent migmatites. They could not intrude the already crystallized, tonalitic Fusht complex which formed a rigid body within the partially molten Sadh complex. They do not even appear in the Hadbin complex because they were consumed by the simultaneous magmatic activity of the Hadbin magmas.

Based on the interfering model, the following scenario for the geologic history of the Hadbin area is proposed.

Figure 8a demonstrates the magmatic setting within a subduction zone, which remained the same during phases I to IV (Figs 8 b-e). Figures 8 b-e can be inserted into the frame within figure 8a.

- *Phase I (Fig. 8b): Pre-Fusht polymagmatic and polymetamorphic history of the Sadh complex.* Calc-alkaline magmas accreted in the lower crust. Syn- and post-intrusive deformation, and high-grade metamorphism produced the typical banded structures of the Sadh complex. U-Pb zir-

con ages, interpreted as crystallization ages, from the Mahall (named after waterhole Mahall; for localization see figure 1) and Sadh complexes cluster closely around 800 Ma (FREI et al., in prep.). The Mahall complex intrudes the Sadh complex (WÜRSTEN, 1994). Thus, this age represents the minimum age of the Sadh complex. Because the Mahall complex is more deformed and, therefore, interpreted to be older than the Fusht complex, this age represents a maximum age of the Fusht complex (phase II).

- *Phase II (Fig. 8c): Intrusion of the Fusht complex into the Sadh complex.* Mantle-derived calc-alkaline dioritic and tonalitic magmas were emplaced during extensive tectonics, favouring fast ascent but impairing crustal contamination.

- *Phase III (Fig. 8d): Final migmatization of the Sadh complex and the contemporaneous early magmatism of the Hadbin complex.* Compressive syn- to post-magmatic tectonics deformed the Fusht complex while calc-alkaline magmas intruded the Sadh complex again. Within this com-

pressive regime, and because of the higher degree of migmatization due to the additional crystallization-heat input by the Fusht complex, the Hadbin magmas ascended slowly and became contaminated by leucogranitic melts of the highly migmatized Sadh complex.

– *Phase IV (Fig. 8e): Final emplacement of the contaminated Hadbin pluton next to the Fusht complex.* The highly migmatized rocks of the Sadh complex between the two plutons were remobilized producing agmatites and leucogranitic dykes.

– *Phase V (Fig. 8f): Uplift history of the crystalline basement of the Hadbin area and the sedimentary cover.* During uplift the crystalline block suffered retrograde greenschist overprinting. The detailed uplift history is locally variable, but, in general, cooling appears to have been very rapid (FREI et al., in prep.). Lamprophyric dyke swarms, interpreted as mantle derivatives, intruded in a brittle environment, indicating that most of the uplift had already taken place by that time. They might be related to the rhyolitic subvolcanics cropping out about 20 km west of the studied area. The intrusion age of these subvolcanics is around 550 Ma (LE METOUR et al., in prep.). After several hydrothermal alteration events the basement was uplifted to the surface where it was covered by Paleozoic sediments near Mirbat (~ 50 km WSW of Hadbin). The upper Cretaceous and Tertiary sediments of the Umm Er Rhadhuma formation overlie the basement of the whole Salalah area.

Our model proposed for the Hadbin area is consistent with both geologic data and interpretations of the Arabian shield. The genesis of this shield is believed to result from the accretion of microplates and the subduction of their intervening oceans, leading to mainly calc-alkaline magmatism and ophiolitic sutures.

The largest exposed part of the Arabian shield is situated in the western and southern parts of the Arabian Peninsula. It consists of volcano-sedimentary successions and associated plutonic complexes, mostly younger than 900 Ma. Plutons with ages between 900 and 680 Ma show mainly tholeiitic to calc-alkaline trends similar to the Fusht and Hadbin complexes. Diorite-tonalite-granodiorite suites are typical for long-standing subduction zones where magma generation in the mantle wedge plays a dominant role (ATHERTON and SANDERSON, 1985). Younger, intrusive rocks with ages between 680 and 550 Ma are calc-alkaline to alkaline (DRYSDALL et al., 1986).

Similar lithologies and rock ages are found in the two erosional windows that expose the crystalline basement in the Jabal J'alan area and the

Huqf area of Oman. In the Jabal J'alan area, calc-alkaline intrusive rocks show ages between 820 and 870 Ma (WÜRSTEN et al., 1991). In the Huqf area, alkaline rhyolites are about 550 Ma old (LE METOUR et al., in prep.). Further evidence for late alkaline magmatism found west of the Hadbin area is a small granitic body and rhyolitic dykes. These probably intruded simultaneously with the lamprophyric dykes of the whole Salalah area.

Acknowledgements

Mohammed Bin Hussain Bin Kassim, Director General of Minerals, and Dr. Hilal Al Azry, Director of Geological Surveys, Ministry of Petroleum and Minerals, Muscat, Sultanate of Oman, are thanked for giving us the possibility to work in Oman. We thank Dr. Hayat A. Qidwai and Dr. Mohd. Ishaq Khalifa, Ministry of Petroleum and Minerals, Southern Region, Salalah, Sultanate of Oman, for their co-operation and assistance.

This study was initiated and directed by Prof. Tjerk Peters and Dr. Ivan Mercolli. We would like to thank them for their solid introduction to the field work and for their help and discussions during this study. Thanks go also to B. Bonin, A. Rottura, J.D. Kramers, F. Würsten, L. Diamond, E. Gnos, M. Handy, D. Kurz, V. Barbin, B. Schwizer, S. Häusler, J. Chermak, L. Bobade, R. Allenbach, M. Janowiak, R. Rüttimann, V. Jakob and J. Megert for stimulating discussions, linguistic reviews and thin section preparations, and to the people of Hadbin for their hospitality during our three months of field work.

References

- ATHERTON, M.P. and SANDERSON, M.L. (1985): The chemical variation and evolution of the super-units of the segmented Coastal Batholith. In: W.S. PITCHER, M.P. ATHERTON, E.J. COBBING and R.D. BECKINSALE (eds): *Magmatism at a plate edge. The Peruvian Andes*. Blackie, Glasgow and London, 1985, 208–227.
- BEYDUN, Z.R. (1966): *Geology of the Arabian Peninsula – Eastern Aden Protectorate and part of Dhufar*. U.S. Geol. Surv. Prof. Paper, 560-H, P. H1-49.
- CASTRO, A., MORENO-VENTAS, I. and DE LA ROSA, J.D. (1991): H-type (hybrid) granitoids: a proposed revision of the granite-classification and nomenclature. *Earth-Science Reviews*, 31, 237–253.
- DRYSDALL, A.R., RAMSAY, C.R. and STOESER, D.B. (1986): Introduction. *Journal of African Earth Sciences*, 4, 1–9.
- GASS, G., RIES, A.C., SHACKLETON, R.M. and SMEWING, J.D. (1990): Tectonics, geochronology and geochemistry of the Precambrian rocks of Oman. From: A.H.F. ROBERTSON, M.P. SEARLE and A.C. RIES (eds): *The geology and tectonics of the Oman region*. Geological Society Special Publication, 49, 585–599.
- HAUSER, A. and ZURBRIGGEN, R. (1992): *Geology of the crystalline basement of the Hadbin area (Salalah area, Dhofar, Sultanate of Oman)*. Diploma thesis, University of Berne, Switzerland.

- ISHIHARA S. (1981) The granitoid series and mineralization. *Economic Geology*, 75th Anniversary Volume, 458–484.
- LE METOUR, J.L.M., KRAMERS, J.D. and FREI, R. (in prep.): Radiometric dating of the beginning of sedimentation on the crystalline basement of the Dhofar and Huqf areas, Oman.
- LAMEYRE, J. and BOWDEN, P. (1982): Plutonic rock types series: Discrimination of various granitoid series and related rocks. *Journal of Volcanology and Geothermal Research*, 14, 169–186.
- METAL MINING AGENCY OF JAPAN, JAPAN INTERNATIONAL COOPERATION AGENCY and GOVERNMENT OF JAPAN (MMAJ, JICA and GJ) (1981): Report on geological survey of the Sultanate of Oman (Salalah area), phase 1. Ministry of Petroleum and Minerals, Sultanate of Oman.
- MOORE, N.D. and AGAR, R.A. (1985): Variations along a batholith: the Arequipa segment of the Coastal Batholith of Peru. In: W.S. PITCHER, M.P. ATHERTON, E.J. COBBING and R.D. BECKINSALE (eds): *Magmatism at a plate edge. The Peruvian Andes*. Blackie, Glasgow and London, 1985, 108–118.
- PEARCE, J.A., HARRIS, N.B.W. and TINDLE, A.G. (1984): Trace element discrimination for the tectonic interpretation of granitic rocks. *Journal of Petrology*, 25/4, 956–983.
- PITCHER, W.S., ATHERTON, M.P., COBBING, E.J. and BECKINSALE, R.D. (1985): A model for the Coastal Batholith. In: W.S. PITCHER, M.P. ATHERTON, E.J. COBBING and R.D. BECKINSALE (eds): *Magmatism at a plate edge. The Peruvian Andes*. Blackie, Glasgow and London, 1985, 239–240.
- ROGER, J. and PLATEL, J.P. (1987): Geological mapping and mineral exploration program in southern Dhofar (Final report). Bureau de Recherches Géologiques et Minières, Orléans, France.
- STRECKEISEN, A.L. (1975): To each plutonic rock its proper name. *Earth-Science Reviews*, 12, 1–33.
- WÜRSTEN, F., FLISCH, M., MICHALSKI, I., LE METOUR, J., MERCOLLI, I., MATTHAEUS, U. and PETERS, Tj. (1991): The uplift history of the Precambrian crystalline basement of the Jabal J'alan (Sur area). From: Tj. PETERS, A. NICOLAS and R.G. COLEMAN (eds): *Ophiolite genesis and evolution of the oceanic lithosphere*. Kluwer Academic Publisher, Dordrecht/Boston/London, 1991, 613–626.
- WÜRSTEN, F. (1994): The Precambrian crystalline basement of Salalah (Dhofar area, Sultanate of Oman). Ph. D. Thesis, University of Berne, Switzerland.

Manuscript received January 11, 1993; revised manuscript accepted January 4, 1994.